International Conference on Applied Energy 2021
Nov. 29 - Dec. 5, 2021, Thailand/Virtual
Paper ID: 245

Spatio-Temporal Coordination of Flexibility Supply in Distributed Energy Systems Based on an Exergy-based Flexibility Cost Indicator

Huan Ma[1], Qinghan Sun[1], Qun Chen[1,2*]

1 Key Laboratory for Thermal Science and Power Engineering of Ministry of Education, Department of Engineering Mechanics, Tsinghua University, Beijing 100084, China

2 State Key Laboratory of Control and Simulation of Power Systems and Generation Equipments, Department of Electrical Engineering, Tsinghua University, Beijing 100084, China

ABSTRACT

Demand-side flexibility in distributed energy systems has aroused broad attention in recent years. However, existing researches are confined to qualitative descriptions or posterior evaluations on flexibility improvement, but the insightful physical mechanism of how and at what cost the distributed energy system offers flexibility is still unclear, especially when it is involved with multi-energy converters and storage. This paper introduces an exergy-based indicator to quantify the cost associated with flexibility improvement of distributed energy systems, then figures out different mechanisms of flexibility improvement of multi-energy storage and converters contributing to the whole energy system. Finally, a spatio-temporal coordination principle for distributed energy systems is established. Results show that the proposed principle is in good agreement with simulation.

Keywords: distributed energy system, multi-energy converters and storage, spatio-temporal coordination principle, flexibility cost, exergy analysis

1. INTRODUCTION

The increased deployment of renewable energy (RE), along with its fluctuating nature and limited time coincidence with power demand, has raised a great requirement of system flexibility [1]. Meanwhile, with the ongoing transformation of energy system from a centralized architecture to a more decentralized one[2], the potential of demand side flexibility in distributed energy systems (DESs) arouses broad attention. A DES usually consists of multi-energy storage devices and different energy converters such as heat pumps (HPs) and combined heat and power (CHP) generators [3], which make it possible to offer demand response by switching the sources of consumed energy, e.g. electricity, thermal energy, natural gas, without compromising the comfort of inelastic users [4]. However, due to different configurations, DESs have diversified flexibility characteristics, which might compete against each other at varying conditions. Thus, the necessity of a dynamic flexibility qualification method to enable the comparison among different flexibility options is evident.

Among different flexibility qualification methodologies, both top-down and bottom-up approaches have been widely adopted from different viewpoints. In the top-down approaches, the flexibility of a prosumer is usually defined as the overall energy supply/demand functions of the electricity selling/purchasing price [5], which neglects intrinsic energy conversion behaviors and has oversimplified assumptions about the demand elasticity. In the bottom-up approaches, the operation characteristics and flexibility performance are modeled and discussed meticulously on different options, ranging from electric heating and cooling [6], heat boiler (HB) [7] to building envelope [8].

Despite of the remarkable contributions, there are still major hindrances that may restrict the further application of existing researches:

(1) In terms of perspective, most of the researches have concentrated on the range characterization of power regulation, with little attention to the potential costs associated with flexibility improvement. As noted

by De Coninck and Helsen [9], flexibility from the demand side is not for free, and the costs of flexibility should be taken into account especially when it is coupled with thermal systems.

(2) Many studies have conducted energy system analysis based on the 1st law of thermodynamics. However, it is only marginally effective and even misleading in the description of an energy system [10], because it cannot discern between low- (heat) and high-quality (power, work) energy flows. Therefore, to provide an insightful assessment of both energy quantity and quality losses associated with flexibility improvement, an analytical indicator based on the 2nd law of thermodynamics is highly required.

To the best of our knowledge, few studies have succeeded in coping with the problems above simultaneously. This paper fills the gap by establishing an exergy-based indicator to evaluate the flexibility cost of DES, and figures out the underlying mechanisms of how the multi-energy converters and storage contribute to the overall flexibility and energy efficiency. Based on the mechanisms, a spatio-temporal coordination principle is proposed to direct the operation of DESs.

2. *SYSTEM DESCRIPTION*

Fig. 1 shows the schematic structure of a typical DES. The power load is met by CHP, PV and purchased power from power grid, and solar heat collector (SHC), CHP, HP and auxiliary HB satisfy the heat load simultaneously. In addition, the system flexibility is further enhanced by heat storage (HS) device. The power and gas flows are expressed as unidirectional arrows, while the heat is transported though the supply and return water pipelines of heating network.

To give a more explicit picture on the energy conversion characteristics, the power and heat balance constraints are

$$P_{CHP,t} - P_{HP,t} = P_{net\_load,t} \tag{1}$$

$$H_{CHP,t} + H_{HP,t} + H_{HB,t} = H_{net\_load,t} \tag{2}$$

where P and H are the power and heat generation (or consumption for HP), the subscript *net_load* denotes the net power or heat loads satisfied by the energy converters, which are defined as:

$$P_{net\_load,t} = P_{load,t} - P_{PV,t} - P_{grid,t} \tag{3}$$

$$H_{net\_load,t} = H_{load,t} - H_{SHC,t} + H_{HS,t} \tag{4}$$

where the subscripts *load*, *grid* and *HS* denote the power or heat loads, the power purchased from the power grid and the net HS rate of the HS device.

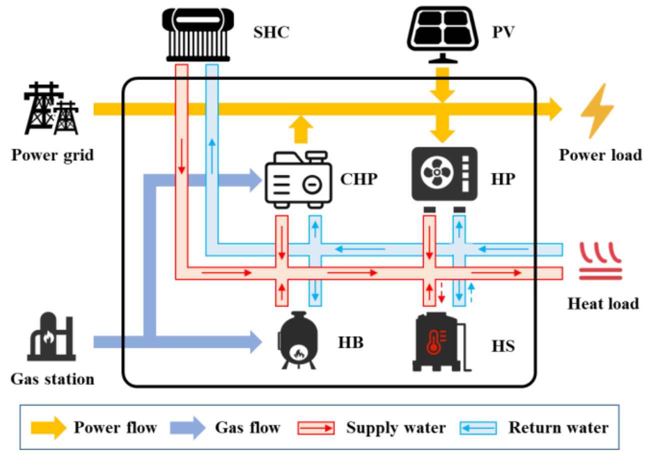

Fig. 1. The schematic structure of a DES

The operation of the energy converters is constrained by

$$\underline{P_{CHP}} \le P_{CHP,t} \le \overline{P_{CHP}} \tag{5}$$

$$0 \le H_{CHP,t} \le \alpha P_{CHP,t} \tag{6}$$

$$0 \le P_{HP,t} \le \overline{P_{HP}} \tag{7}$$

$$H_{HP,t} = \beta P_{HP,t} \tag{8}$$

$$0 \le H_{HB,t} \le \overline{H_{HB}} \tag{9}$$

where the overline and underline represent the upper and lower limits respectively, α and β are the maximum heat-to-power ratio of CHP and the coefficient of performance (COP) of HP, respectively. Here, Eq. (6) enables possible heat discarding of CHP by the form of inequality, and the CHP generator would operate at the power-only mode when $H_{CHP,t} = 0$.

The operation of HS device is constrained by:

$$-\overline{H_{HS,t}} \le H_{HS,t} \le \overline{H_{HS,t}} \tag{10}$$

$$Q_{t+1} = Q_t + H_{HS,t}\Delta T \tag{11}$$

$$0 \le Q_t \le \overline{Q} \tag{12}$$

$$Q_0 = Q_T = 0.5\overline{Q} \tag{13}$$

where the negative and positive $H_{HS,t}$ represent the heat release (HR) and HS modes respectively, Q is state of charge of HS device , ΔT is the time interval, the subscripts *0* and *T* denote the start and end time slots of the dispatch periods.

The natural gas consumption is expressed as

$$G_{CHP,t} = \frac{(1+\alpha)P_{CHP,t}}{\eta_0 q} \tag{14}$$

$$G_{HB,t} = \frac{H_{HB,t}}{\eta_0 q} \tag{15}$$

where G is the natural gas consumption, η_0 and q are the maximum efficiency based on the 1st law of thermodynamics and the calorific value of natural gas respectively.

While the first law generally fails to identify the loss of energy quality and the effective use of resources, the second law of thermodynamics could depict that in an irreversible process, the quantity of energy is conserved but the quality (i.e., the exergy) disperses. Neglecting exergy destruction in the combustion process, the total input and output exergy of the energy converters are calculated as [11]:

$$E_{in,t} = q\left(G_{CHP,t} + G_{HB,t}\right)\left(1 - \frac{T_0}{T_b}\right) \quad (16)$$

$$\begin{aligned} E_{out,t} &= \sum_{i=CHP,HP,HB} \left(E_{i,s,t} - E_{i,r,t}\right) + P_{net\_load,t} \\ &= \sum_{i=CHP,HP,HB} m_{i,t} c \left(T_s - T_r - T_0 \ln \frac{T_s}{T_r}\right) + P_{net\_load,t} \\ &= \sum_{i=CHP,HP,HB} H_{i,t} \left(1 - \frac{T_0}{T_s - T_r} \ln \frac{T_s}{T_r}\right) + P_{net\_load,t} \\ &= H_{net\_load,t} \left(1 - \frac{T_0}{T_s - T_r} \ln \frac{T_s}{T_r}\right) + P_{net\_load,t} \end{aligned} \quad (17)$$

where *E*, *m*, *c* and *T* denote exergy, mass flow rate and specific heat capacity of the circling water, and temperature respectively, the subscripts *in*, *out*, *0*, *b*, *s* and *r* denote the total input and output exergy, environment temperature, gas burning temperature, supply and return water temperatures respectively. Here, the supply and return water temperatures of each converter are assumed constant, and their heat loads are regulated with the adjustment of $m_{i,t}$.

3. *QUALIFYING MULTI-ENERGY FLEXIBILITY AND ITS COST*

3.1 Definition and qualification of multi-energy flexibility

In a power system context, the flexibility is regarded as the ability to modify power generation or consumption in response to the fluctuation of power load or RE [12]. However, in the context of multi-energy, it is suggested that the flexibility should be discussed in both the power and heat dimensions.

Define the feasible region of the energy converters as the convex polyhedron:

$$\Omega_t = \left\{x_t \,\middle|\, Eqs.(5)-(9)\right\} \quad (18)$$

where,

$$x_t = \left(P_{CHP,t}, H_{CHP,t}, P_{HP,t}, H_{HP,t}, H_{HB,t}\right) \quad (19)$$

Then, the multi-energy flexibility of the energy converters is defined as the feasible region of total power and heat outputs, which is mathematically the projection of Ω_t onto the subspace ($P_{net\_load,t}$, $H_{net\_load,t}$):

$$\Theta_t = \left\{y_t \,\middle|\, Eqs.(1)-(2), x_t \in \Omega_t\right\} \quad (20)$$

where,

$$y_t = \left(H_{net\_load,t}, P_{net\_load,t}\right) \quad (21)$$

To solve the projection, the vertex-oriented algorithm can be adopted. The basic idea is that the projection of a convex polyhedron could be regarded as a convex hull of the projections of polyhedron vertices, where a general vertex enumeration algorithm for high-dimensional problems can refer to [13]. Based on this method, the scope of multi-energy flexibility could be qualified, as illustrated in Fig. 2.

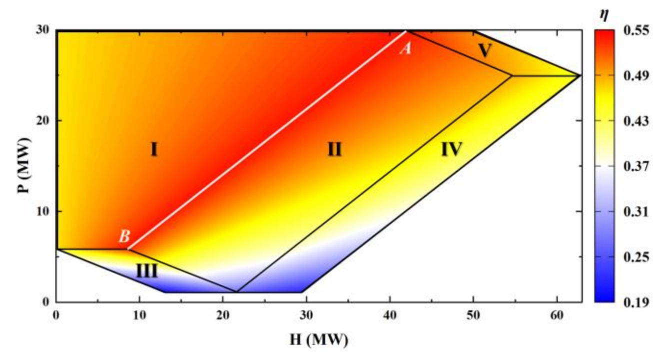

Fig. 2. The scope of multi-energy flexibility and the distribution of 2nd law efficiency

3.2 The cost associated with multi-energy flexibility

To capture the dynamic cost when the energy converters offer multi-energy flexibility, an exergy-based optimization under different power and heat conditions is conducted. The optimal input exergy could be expressed as:

$$E^*_{in,t}\left(y'\right) = \min_{x_t} \left\{\begin{array}{l} E_{in,t}\left(x_t\right): \\ s.t. \quad x_t \in \Omega_t, \\ \qquad y_t = y', \\ \qquad Eqs.(1)-(2) \end{array}\right\}, \forall y' \in \Theta_t \quad (22)$$

where *y'* is the given total power and heat conditions of energy converters. Denote the optimal operation as $x_t^*(y')$, and define the exergy efficiency base on the 2nd law of thermodynamics as:

$$\eta\left(y'\right) = \frac{E_{out,t}\left(y'\right)}{E^*_{in,t}\left(y'\right)}, \forall y' \in \Theta_t \quad (23)$$

Plot the distribution of η in the scope of Θ as Fig. 2. It indicates that the maximum energy efficiency is achieved when the energy converters operate on the line *AB*. On the line *AB*, only the CHP operate, where

$$x_t \in \left\{ \left(P_{CHP,t}, \alpha P_{CHP,t}, 0, 0, 0 \right) \middle| \underline{P_{CHP}} \le P_{CHP,t} \le \overline{P_{CHP}} \right\} \quad (24)$$

$$y_t \in \left\{ \left(P_{CHP,t}, \alpha P_{CHP,t} \right) \middle| \underline{P_{CHP}} \le P_{CHP,t} \le \overline{P_{CHP}} \right\} \quad (25)$$

By substituting (24)-(25) into Eqs. (14)-(17) and (23), the maximum energy efficiency on the line *AB* could be calculated as:

$$\eta^* = \frac{\eta_0 \left(\alpha\lambda + 1 \right)}{\left(1 + \alpha \right) \left(1 - \frac{T_0}{T_b} \right)} \quad (26)$$

where,

$$\lambda = 1 - \frac{T_0}{T_s - T_r} \ln \frac{T_s}{T_r} \quad (27)$$

Beyond the operation on the line *AB*, the energy converters would endure the efficiency decrease. Set η^* as a benchmark efficiency, and define the additional exergy destruction as:

$$E_{AED}\left(y' \right) = E_{in,t}^*\left(y' \right) - \frac{E_{out,t}\left(y' \right)}{\eta^*}, \forall y' \in \Theta_t \quad (28)$$

where the subscript *AED* denotes the additional exergy destruction comparing with the benchmark conditions on the line *AB*.

As illustrated in Fig. 3, the additional exergy destruction emerges as a quantitative indicator of the cost associated with multi-energy flexibility improvement. For the energy converters, the most efficient operations lie on the line *AB*, and offering more multi-energy flexibility implies exposing the energy converters to additional exergy destruction.

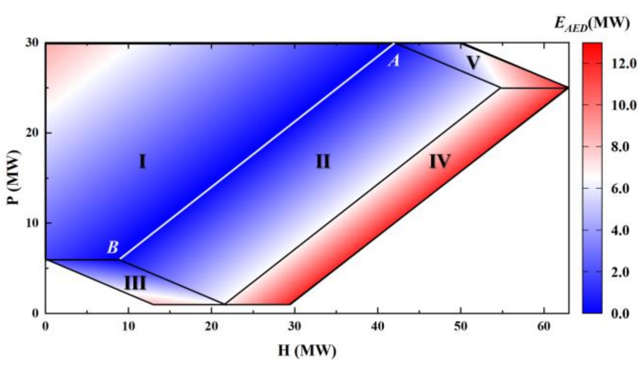

Fig. 3. The distribution of additional exergy destruction

According to the operational combinations of energy converters in $x_t^*(y')$, the whole area in Fig. 3 could be divided into 5 regions. In each region, the corresponding operational combinations are listed as Table 1.

Denote the gradient of additional exergy destruction as $\left[\frac{\partial E_{AED}}{\partial H}, \frac{\partial E_{AED}}{\partial P}\right]$, which mathematically represents the marginal costs of flexibility improvement in directions of both heat and power.

Table 1 The operational combinations of energy converters

Regions	*CHP*		*HP*	*HB*
	P_{CHP}	H_{CHP}	P_{HP}	H_{HB}
I	$[\underline{P_{CHP}}, \overline{P_{CHP}}]$	$[0, \alpha \underline{P_{CHP}}]$	0	0
II	$[\underline{P_{CHP}}, \overline{P_{CHP}}]$	αP_{CHP}	$[0, \overline{P_{HP}}]$	0
III	$\underline{P_{CHP}}$	$[0, \alpha \underline{P_{CHP}}]$	$[0, \overline{P_{HP}}]$	0
IV	$[\underline{P_{CHP}}, \overline{P_{CHP}}]$	αP_{CHP}	$\overline{P_{HP}}$	$[0, \overline{H_{HB}}]$
V	$\overline{P_{CHP}}$	$\alpha \overline{P_{CHP}}$	$[0, \overline{P_{HP}}]$	$[0, \overline{H_{HB}}]$

For DESs, the most efficient choice is to operate on the line AB. As for RE plants, the most efficient choice is to accommodate all the available power, otherwise the whole integrated energy system would suffer an additional exergy loss of 1 MW for every MW abandoned RE availability. However, the optimal operations of DESs and RE can be hardly achieved at the same time because of power balance requirement and the volatility of loads and RE. Thus, it requires great collaboration of DESs to maximize the overall efficiency.

4. *THE IMPACT OF HEAT STORAGE ON THE FLEXIBILITY AND EFFICIENCY*

The operation of HS has been excluded from the discussion about energy converters thus far. Now that a quantitative indicator about multi-energy flexibility is available, we can reassess the impact of HS on the flexibility and efficiency of DESs.

It has been extensively discussed in the literature that HS could further expand the range of flexibility by shifting the equivalent heat load of energy converters. However, the mechanism of how the HS contributes to the overall efficiency is rarely analyzed.

As a contrast, the proposed indicator gives a readily visualizable interpretation in Fig. 4 that the HS benefits

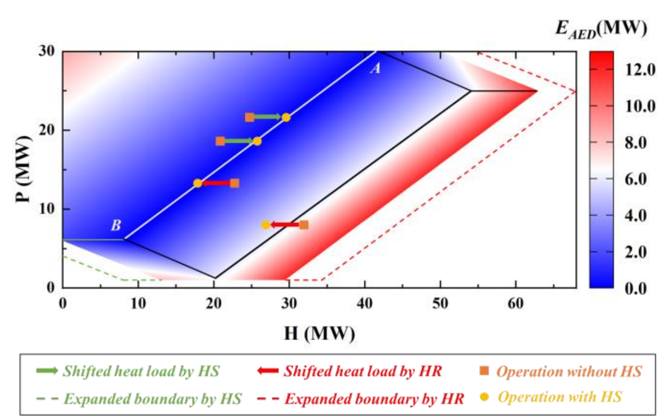

Fig. 4. The impact of HS on the energy converters

DESs in at least 2 ways: (1) Further expand the range of flexibility; (2) Compensate for part of the additional exergy destruction caused by flexibility improvement. Specifically, with the adjustment of HS and HR, the heat loads could be reallocated in the temporal dimension and energy converters could shift their operation towards the decrease of additional exergy destruction.

5. *A SPATIO-TEMPORAL COORDINATION PRINCIPLE*

Suppose there is an integrated energy system consisting of multiple DESs and RE plants. In the spatial dimension, DESs all over the power grid offer power flexibility at a certain cost of additional exergy destruction to compensate for RE fluctuation. In the temporal dimension, the HS compensates for the additional exergy destruction by reallocating the heat loads at different periods.

By comparing the coordination in the spatial and temporal dimensions, interesting similarities and distinctions can be drawn. Both the objectives are to minimizie the overall exergy destruction, but the regulating directions are starkly orthogonal (i.e., along the power and heat directions respectively). The feature above enables the decomposed spatio-temporal coordination of integrated energy systems, which consists of main steps in the following flowchart.

	The decomposed spatio-temporal coordination principle
1	**Initialization:** Supposing there is no HS. **for** *k* **do** Initialize the operations of DES *k* on the line AB: ($H^k_{net\_load,t}/\alpha$, $H^k_{net\_load,t}$)

2	**for** *t* **do**
	if $\sum_k P_{grid,t} < P_{RE,t}$, there is RE curtailment, **then**
	DESs offer downward power flexibility by the ascending order of marginal cost $\left(-\frac{\partial E_{AED}}{\partial P}\right)_{k,t}$ until RE curtailment is eliminated or reaching power flow limits.
	else, there is power shortage, **then**
	DESs offer upward power flexibility by the ascending order of marginal cost $\left(\frac{\partial E_{AED}}{\partial P}\right)_{k,t}$ until power shortage is eliminated or reaching power flow limits.

3	**for** *k* **do** Shift $H^k_{net\_load,t}$ $(t \in [0, 1, \dots, T])$ towards the line AB by the descending order of $\left|\frac{\partial E_{AED}}{\partial H}\right|_{k,t}$ under the temporal constraints (10)-(13) of HS facility in DES *k*.

Assumptions: for brevity of illustration, η_0, α and λ among distributed energy systems are assumed the same so that their benchmark efficiencies could remain consistent.

6. *RESULTS AND DISCUSSIONS*

6.1 Qualification of multi-energy flexibility in DES and its marginal costs

Apply the proposed method in section 3 to the DES in Fig. 1, where the related parameters are available at [14]. The scope of multi-energy flexibility and distribution of additional exergy destruction could be found in Fig. 3. Besides, the marginal costs of flexibility improvement are mathematically the gradients of additional exergy destruction in different regions, which are calculated and then listed as Table 2.

Table 2 The marginal costs of flexibility improvement

Regions	$\left[\frac{\partial E_{AED}}{\partial H}, \frac{\partial E_{AED}}{\partial P}\right]$
I	[-0.2070, 0.2898]
II	[0.3274, -0.4584]
III	[-0.2070, -1.8477]
IV	[0.6836, -0.9570]
V	[0.6836, 0.4677]

Especially, for every MW downward power flexibility in Region III, the energy converters will undertake an additional exergy destruction of 1.8477 MW, which is exactly equivalent to $1/\eta^*$=1/0.5412=1.8477 MW. Noting that the cost exceeds the income of 1 MW RE accommodation, offering downward power flexibility in Region III would never be efficiency-effective.

In addition, the marginal cost of downward power flexibility in Region IV is more than twice that of Region II. Combined with Table 1, it could be inferred that HB would cause much larger efficiency loss than HP. As 2 of the auxiliary heating options, HP is superior to HB at most conditions.

6.2 The spatio-temporal coordination

Consider the 5-bus integrated energy system in Fig. 5, where DES1 is the same as Fig. 1, DES3 is a traditional power consumer. Besides, the parameters, scope of multi-energy flexibility, distribution of additional exergy destruction and marginal costs of flexibility improvement of DES2 are listed in the on-line supplementary material [14]. It is worth noting that the HP of DES2 has a higher β than that of DES1, so DES2 has a lower marginal cost when offering downward power flexibility in Region II.

Optimize the reference simulation case that we minimize the total gas consumption of the 5-bus integrated energy system by directly solving the spatio-temporal coupling optimization. Then apply the

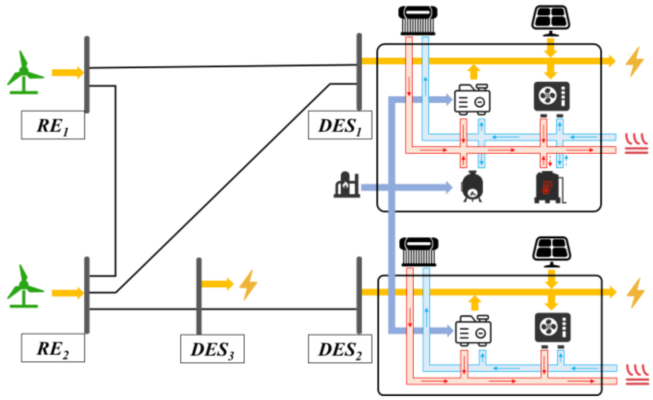

Fig. 5. A 5-bus integrated energy system

proposed spatio-temporal coordination, and compare the results with those from the reference case. As shown in [14], the maximum difference of power generation is no more than 0.15 MW, and the results are in good agreement. The results also reveal that DES2 has a priority for offering downward power flexibility over DES1, which is exactly consistent with the relation between their marginal costs in Region II.

7. *CONCLUSIONS*

A novel exergy-based indicator, the additional exergy destruction, is proposed to quantify the cost associated with flexibility improvement in DESs. Based on the indicator, the mechanism of how the multi-energy converters and storage contribute to the overall flexibility and energy efficiency could be analyzed. In the spatial dimension, DESs offer power flexibility at the cost of additional exergy destruction to improve the overall efficiency of integrated energy system. In the temporal dimension, the HS device compensates for part of the additional exergy destruction with the adjustment of HS and HR. According to the mechanisms, a decomposed spatio-temporal principle is proposed to direct the coordination of DESs. In contrast with directly solving the spatio-temporal coupling optimization, the proposed mechanism-based principle helps to clarify the contribution of each component, and applies to more large-scale system due to its decomposed nature in spatio-temporal dimensions.

ACKNOWLEDGEMENT

The work is supported by the National Natural Science Foundation of China (Grant No. 51836004).

REFERENCE

[1] Denholm P, Hand M. Grid flexibility and storage required to achieve very high penetration of variable renewable electricity. Energy Policy. 2011;39:1817-30.

[2] Burger C, Froggatt A, Mitchell C, Weinmann J. Decentralised Energy: A Global Game Changer. London: Ubiquity Press; 2020.

[3] Sheikhi A, Rayati M, Bahrami S, Ranjbar AM. Integrated Demand Side Management Game in Smart Energy Hubs. IEEE Transactions on Smart Grid. 2015;6:675-83.

[4] Wang J, Zhong H, Ma Z, Xia Q, Kang C. Review and prospect of integrated demand response in the multi-energy system. Applied Energy. 2017;202:772-82.

[5] Wang Z, Yu X, Mu Y, Jia H, Jiang Q, Wang X. Peer-to-Peer energy trading strategy for energy balance service provider (EBSP) considering market elasticity in community microgrid. Applied Energy. 2021;303:117596.

[6] Arteconi A, Mugnini A, Polonara F. Energy flexible buildings: A methodology for rating the flexibility performance of buildings with electric heating and cooling systems. Applied Energy. 2019;251:113387.

[7] Stinner S, Huchtemann K, Müller D. Quantifying the operational flexibility of building energy systems with thermal energy storages. Applied Energy. 2016;181:140-54.

[8] Reynders G, Diriken J, Saelens D. Generic characterization method for energy flexibility: Applied to structural thermal storage in residential buildings. Applied Energy. 2017;198:192-202.

[9] De Coninck R, Helsen L. Quantification of flexibility in buildings by cost curves – Methodology and application. Applied Energy. 2016;162:653-65.

[10] Sciubba E. Exergy Destruction as an Ecological Indicator. In: Jørgensen SE, Fath BD, editors. Encyclopedia of Ecology. Oxford: Academic Press; 2008. p. 1510-22.

[11] Wall G. Exergy and Exergy Tools☆. Reference Module in Earth Systems and Environmental Sciences: Elsevier; 2013.

[12] Fischer D, Wolf T, Wapler J, Hollinger R, Madani H. Model-based flexibility assessment of a residential heat pump pool. Energy. 2017;118:853-64.

[13] Avis D, Fukuda K. A pivoting algorithm for convex hulls and vertex enumeration of arrangements and polyhedra. Discrete & Computational Geometry. 1992;8:295-313.

[14] Supplementary material. Available: https://cloud.tsinghua.edu.cn/d/e638f8362e8a49b6a5a8/

